Validation of the Dynamic Wake Meander Model with AREVA M5000 Load Measurements at alpha ventus

Björn Schmidt[1] Ursula Smolka[2] Sebastian Hartmann[3] Po Wen Cheng[2]

8.2 Consulting AG[1]
Brandstwiete 4
20457 Hamburg, Germany
Tel: +49 (0)40 3807 253-31
Fax: +49 (0)40 3807 253-99
bjoern.schmidt@8p2.de

Stuttgart Wind Energy[2]
University of Stuttgart Allmandring 5B
70569 Stuttgart, Germany
Tel: +49 (0)711 685-68255
Fax: + 49 (0)711 685-68293
smolka@ifb.uni-stuttgart.de

AREVA Wind GmbH[3]
Am Lunedeich 156
27572 Bremerhaven, Germany
Tel: +49 (0) 471 8004-5973
Fax: +49 (0) 471 8004-100
sebastian.hartmann@areva.com

Abstract

The Dynamic Wake Meandering (DWM) model was developed for wake load simulations in on- and offshore wind farms. The present paper outlines the DWM model and describes its validation with two years of load measurement data obtained from an AREVA M5000-116 turbine in the alpha ventus wind farm.

The validation adds important aspects that have not been validated so far to the previous DWM validations, those include:

- wakes approaching from further distances (10.2 and 16 rotor diameters)
- a partly wider wind speed range from cut-in to 20 m/s
- another wind turbine concept (AREVA M5000-116) and another DWM model implementation (Bladed code)

The DWM load validation for 16 rotor diameters is arguable. The differences between simulation and measurement may be caused by a turbulence underestimation in the input to the DWM simulation or by a DWM model inadequacy for very large spacings. On the other hand, the results shows a good agreement between measured and simulated fatigue load components of the blade and the tower for the relatively large spacing of 10.2 rotor diameters, confirming the full-scale load validations in [12] and [10] for lower spacings.

The fully calibrated 360° measurements reveal that the wake loads can be significantly above a spacing of 10 rotor diameters. This is in contrast with the common standard approach of the industry, consultants and certification agencies to consider wake loads up to a spacing of 10D.
The DWM model can be considered ready for evaluation against the effective turbulence model which might lead to a refined design process with a positive economic impact. Presently, the DWM model is discussed for inclusion in the edition 4 of the IEC 61400-1 Standard that is planned to be published in 2015.

Disclaimer
The present load validation with AREVA M5000-116 data from the alpha ventus wind farm uses specific data windows. The loads obtained are thus not comparable to the design or certification loads of the AREVA M5000-116 wind turbine or its support structures.

1 Introduction

Wind turbine wakes effect the downstream wind field and increase dynamic loads for downstream turbines. Growing sizes of wind farms, particularly in combination with low ambient turbulence over the sea, significantly increases turbine loading. Thus, the need arose to improve wake load modelling.
One main question governing the analysis of offshore wind farms is whether the wake predictions are conservative and how much room for optimizations exists, especially concerning the designs of the support structure and the park layout.

The actual wake load model for design and certification purposes is the effective turbulence intensity approach. It is suggested in the informative Annex of the IEC 61400-1 Standard [3].
At present, the maintenance team of the IEC Standard discusses another model to be published in a second informative Annex of the coming IEC 61400-1 Standard in edition 4 that is to be published in 2015. That model is the DWM model as presented in the following section.

2 The DWM model

The basic philosophy of the DWM model is a split of scales in the wake flow field, based on the conjecture that only large turbulent eddies are responsible for stochastic wake meandering, whereas the small turbulent eddies are responsible for wake attenuation and expansion in the meandering frame of reference as caused by the turbulent mixing. It is consequently assumed that the transport of wakes in the atmospheric boundary layer can be modelled by considering the wakes to act as passive tracers driven by a combination of large-scale turbulence structures and a mean advection velocity, adopting the Taylor hypotheses.

Illustrating the DWM approach, it can be pictured as being composed of the following three corner stones:

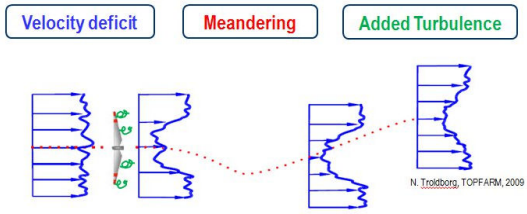

Figure 2.1: The three DWM corner stones

1. **Velocity deficit:** The reduced wind velocity profile behind the rotor that is caused by the extraction of kinetic energy at the rotor plane. (A model of the wake velocity deficit as formulated in the meandering frame of reference).
2. **Meandering:** The movement of the wind speed deficit in space. (A stochastic model of the down-stream wake meandering process).
3. **Added turbulence:** The turbulence inducing creation of blade and hub vortices. (A model of the added wake turbulence, described in the meandering frame of reference).

Detailed descriptions of the various sub-models can be found in [2], [4], [5], [6] and [7]. Within the TOPFARM research project (EU project reference No.: 38641), the DWM model had been developed mainly by Risø DTU [8]. Therein, the DWM model was thoroughly calibrated against Actuator Line (ACL) simulations by H.A. Madsen et. al. [9]. Subsequently, the DWM model was implemented in the wind turbine load simulation code GH Bladed as specified in Chapter 3.
DWM model load validation and comparison versus certification approaches had been performed within TOPFARM [10] and subsequently by the author et. al. [11]. Thereafter, the DWM model was recalibrated with power deficit measurements [12]. The present paper considers the recalibrated DWM model.
The latest load validation was performed with load measurement data obtained from a Vestas V90 3MW turbine in the Egmond aan Zee offshore wind farm [12]. Herein, T.J. Larsen et. al. used the load simulation code HAWC2. The wake situation for the main load validation consisted of several full wakes approaching from a distance of 7 rotor diameters and multiples of that. The results obtained were encouraging, showing a good agreement with the main wake affected loads components [12].

In order to strengthen the confidence in the DWM model, validation of further loading situations was essential and is carried out as documented in the present study, describing a wake load validation with AREVA M5000-116 load measurement data from the alpha ventus offshore wind farm. The analysis code used was a DWM implementation in the load simulation software GH Bladed, as specified in the following.

3 Bladed DWM software

The Bladed DWM module allows a dynamic wake deficit to be superimposed on top of ambient turbulence. The sections below describe the components of the dynamic wake meandering model.

3.1 Meandering generation

Within Bladed, the wind file governing the meandering motion is generated from a low pass filtered turbulence spectrum. The wind file velocities resulting from the inverse Fourier transform of this turbulence spectrum are therefore those associated with the low frequency components of the turbulence. The low pass frequency f_c suggested by Risø [8] for ambient turbulence-wake interaction is defined as:

$$f_c = \frac{U}{2D} \quad (1)$$

U = mean wind speed
D = Rotor diameter of affecting turbine

The low frequency components of the turbulence govern the lateral and vertical transportation of the wake deficit downstream. Since the wind file has been generated to include only the velocities that interact with the wake, no further filtering or processing of the velocities is required. The meandering displacement time history is based on the 'cascade of deficits' model reported by Risø [8]. This assumes a deficit is released at each time step within a frozen turbulent wind field. The transportation of each deficit is governed solely by the velocity that it encounters as it is released into the frozen turbulent wind field. Therefore the lateral y(t) and vertical z(t) displacement at downwind position L_d is equal to:

$$y(t) = v(t) \cdot \left(\frac{L_d}{U} \right) \quad (2)$$

$$z(t) = w(t) \cdot \left(\frac{L_d}{U} \right) \quad (3)$$

v(t) = lateral velocity
w(t) = vertical velocity

3.2 Wake deficit velocity profile and propagation

The existing Eddy Viscosity Model proposed by Ainslie [13] initialises with an induced pressure-expanded velocity deficit. The Ainslie model is based on the thin shear layer approximation of the Navier-Stokes equation. The Reynolds stress terms governing the transfer of momentum from the ambient turbulence to the wake at each downwind position are approximated with an eddy viscosity proportional to the width of the deficit shear layer and the shear velocity gradient.

4 alpha ventus

The present wake load validation is carried out with alpha ventus load measurement data, obtained in the OWEA and the OWEA LOADS research projects for verification of offshore wind turbines. OWEA is part of the EU research framework RAVE (Research at Alpha VEntus).
The alpha ventus offshore wind farm is situated approximately 50km off the German coast in about 30m deep water of the North Sea, as illustrated in Figure 1. The wind farm consists of twelve 5MW turbines.

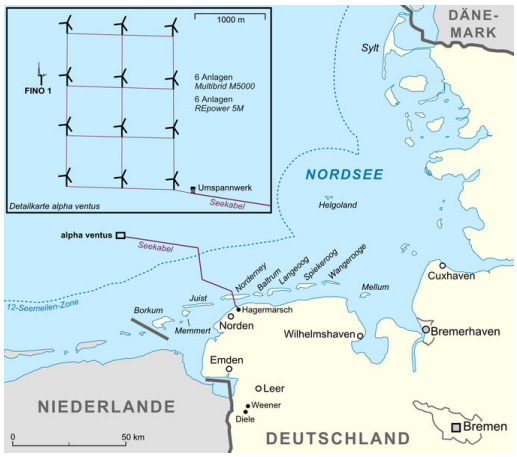

Figure 1: Location of the alpha ventus wind farm.

A zoom into the wake relevant layout of alpha ventus is provided in Figure 2.
The measurement equipped turbine is the AREVA M5000-116 turbine No. AV7, indicated in red. The spacings of the wind turbines towards AV7 are given in multiples of the rotor diameter (D). The met mast is situated to the west of the wind farm.

At the time of the study, 2 years of thoroughly calibrated load measurement data were available from the OWEA and the OWEA LOADS project. This calibration is greatly acknowledged. The data originated from strain gauges at the blade root, the tower top and a sensor close to tower bottom at 7,6m with respect to LAT (lowest astronomical tide) that is referred to as tower bottom

sensor in the following chapters. Due to sensor errors at the blades, the time series of data that are available for blade and tower sensors differs.

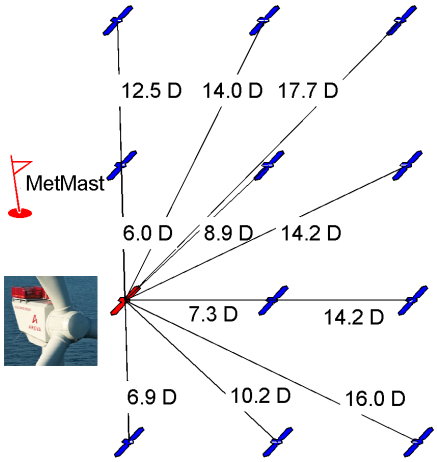

Figure 2: Park geometry with wake distances in rotor diameters (D) to the load measurement equipped AV7 (red) AREVA M5000-116 turbine.

4.1 Wake sectors

The data availability for wake load validation is lower than for freestream situations due to a prevailing wind direction from west-south-west. Due to a period of blade sensor errors, the availability of load measurement data for the tower is higher than for the blade.
Superposing the measurement rose of blade load data with the AV7 turbine within the park layout shows that the only wake situation with a promising amount of load measurement data is the direction with a wake from 16D, see Figure 3.

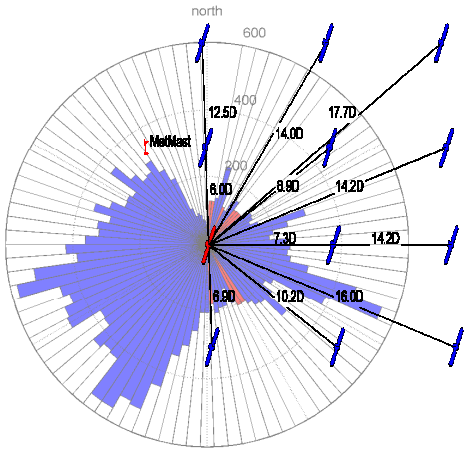

Figure 3: Relating the limiting (due to sensor errors) blade load data rose to the wakes in rotor distances D that affect the AV7 turbine loads.

A more detailed insight revealed that the 10.2D distance has an acceptable data level, as well.
All other wake affected directions do have too little data for the validation purpose, leading to a high statistical uncertainty, especially in the high wind speed region.

5 Freestream validation

The freestream load validation performed herein uses specific data, the loads obtained are thus not anyhow comparable to the loads that are relevant for design or certification of the AREVA M5000-116 wind turbine or its support structure in the alpha ventus farm.

The agreement between simulated and measurement fatigue loading is assessed in free stream conditions, in order to gain confidence in the model used. The main loading components considered are the blade root flapwise bending moment, the tower top yaw moment and the tower base bending moment.
A significant offset between simulated and measured tower top yaw moments appeared. As the reason for this offset could not be identified within a reasonable time period, the yaw torsion load component is not validated in the following considerations, neither for freestream nor for wake conditions.

The simulations are conducted with the AREVA Bladed wind turbine model with location-specific support structure and soil parameters. For each wind bin, 6 stochastic independent 10-min wind time series were simulated.

For the parameterization of the environmental conditions within the simulation setup, 10-minute mean turbulence intensities and logarithmical shear exponents are computed from Fino1 measurements for each 1 m/s wind speed bin. Due to the stiff nature of the support structure and the height difference between waves and tower load sensor, the impact of hydrodynamic loading on the structure is neglected. As the data availability of blade and tower loading differs significantly, separate computation of the prevalent environmental condition is re-

quired. This leads to two distinct simulation parameterizations each accounting for the related disturbances measured at the time the loading data was recorded.

The measured and the simulated resulting 1Hz damage equivalent loads (DEL) along with a wind speed bin-wise computed mean DEL value are depicted in Figure 4 for the blade root flapwise bending moment and in Figure 5 for the tower bottom fore-aft bending moment. The data presented is normalized with the measured mean 1 Hz DEL at a mean wind speed of 10 m/s.

The blade root bending moments (Figure 4) show a very good agreement, considering the conservatism that is provided by the simulation (red) when a filter of ±0.5% around the simulated turbulence intensity is applied. For both tower and blade loads the mean measured DEL curve is lowered due to the removal of (higher) turbulence intensities that are not simulated.

.

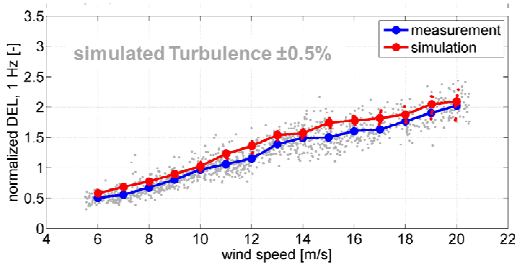

Figure 4: **Freestream – Blade fatigue load**
Mean measured (blue) and simulated (red) freestream blade root flapwise bending moments (DEL, m = 10).
Measured loads limited to turbulence intensities of ±0.5% around simulated ones.

The tower bottom fore-aft moments (Fig. 5) show a good agreement for wind speeds above rated. Below rated, the applied turbulence intensity filter that is meant to restrict measurement data to only those closely corresponding to the simulation setup seems not sufficient to match the mean load level.

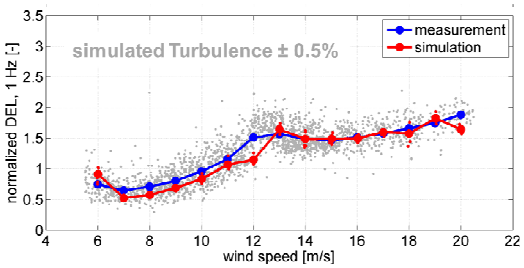

Figure 5: **Freestream – Tower fatigue load 1**
Mean measured (blue) and simulated (red) tower bottom fore-aft bending moments (DEL, m = 4).
Measured loads limited to turbulence intensities of ±0.5% around simulated ones.

Therefore a second filter is applied that limits the tower measurement data to those recorded at a vertical wind shear of ±0.03 around the simulated shear values. As bin-wise wind shear was not used for the full load region simulations, the enhanced agreement is shown in Figure 6 for the partial load region only.

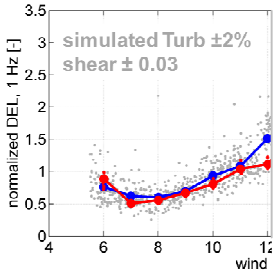

Figure 6: **Freestream – Tower fatigue load 2**
The measured freestream tower bottom fore-aft bending moments are limited to turbulence intensities of ±2% and vertical wind shears of ±0.03 around the simulated ones.

6 Ambient turbulence detection for the wake validation

As stated in Section 4.1, there is a sufficient amount of measurement data available in the sectors between approximately 110° and 140°, with wakes approaching from 16D and 10.2D. In that direction, the met mast is in the wake of several turbines as illustrated in Figure 7.
Due to that, the met mast wind measurement could not be used as a direct turbulence input for the DWM simulations. Consequently, various approaches are studied to allow for a suitable assumption upon the ambient turbulence intensity required for the wake simulation setup.

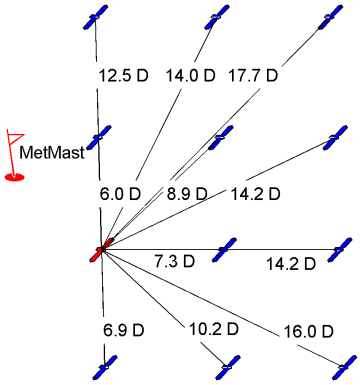

Figure 7: Park geometry with wake distances to AV7 (red) in rotor diameters (D).

In this specific case, the most promising approach showed to be a reconstruction of the ambient turbulence intensity from the nacelle anemometer of turbine AV12. This turbine creates the wake but is in freestream itself.

Out of various approaches, the highest correlation coefficient with R = 0.56 was found for establishing a calibration function for both, the mean wind speed and the standard deviation individually, to subsequently compute the ratio of these values.

Applying the corresponding calibration function to the 16D wake case data, the results in assumed ambient turbulence intensities are given in Figure 8. Considering the relatively high turbulence level of the reconstructed results (R = 0.56) in comparison to measured results from a period before the farm erection [13], the anemometer reconstruction is considered not reliable.

Thus, these values are not used to derive environmental conditions for the simulation setup nor to apply a turbulence intensity filter as has been done for the freestream validation case.

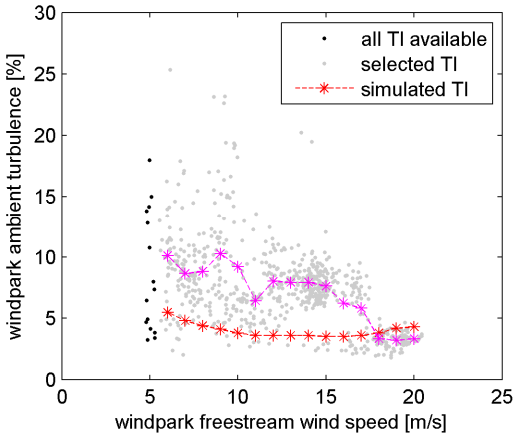

Figure 8: Freestream turbulence intensity reconstructed from nacelle anemometer (grey with mean values in pink), using the calibration method with R = 0.56. Red: Directional (120° sector) 5 year mean values from [13] as used for the wake simulations.

6.1 DWM simulation assumptions

First, the wind direction at which the wake load diminishes to reach ambient loading is estimated. The estimation uses the outcome of a previous parameter study in [1].
Taking the estimated ambient load angle together with the peak load estimation from [1] into account and considering the unequally distributed wake load data (Figure 3), the DWM simulations are carried out for specific direction bins.

Wind shear

Because the met mast is affected by the wake during the considered load measurement periods, the vertical wind shear was assumed to be constant with a wind shear exponent alpha = 0.08 what correlates to the mean value in freestream conditions.

6.1.1 Turbulence

Instead of using an unreliable reconstruction of the turbulence from anemometers, the DWM simulation input is derived from a measurement campaign that was performed before the park erection.
This study by A. Westerhellweg et. al. [13] provides directional 5 year mean turbulence intensities that originate from FINO1 met mast measurements. The data was collected before the alpha ventus wind farm was erected. Although this approach introduces significant uncertainties with respect to the prevalent environmental conditions, this is the closest and most obvious assumption that can be made considering that the met mast measurements are unusable due to the wind farm wake disturbance.
Viewing the study's directional turbulence intensities (Figure 9), the strong directionality in the turbulence intensity should be noted as well as the fact that the dark orange plotted sector of 120° –that is used for the DWM wake load validation in Section 7– represents the sector with the lowest turbulence level (ranging from about 5.5% at 6 m/s to 4% at 20 m/s).

Furthermore, it is worth to notice that such a turbulence level is quite low in relation to other North or Baltic sea wind farms and significantly lower compared to onshore wind farms.

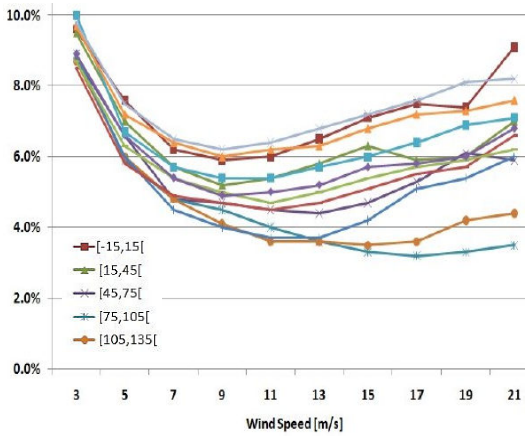

Figure 9: Directional plots of 5y mean turbulence intensities, measured at the FINO1 met mast at 91.5m LAT before the alpha ventus erection [13]

DWM simulation turbulence intensities plotted in dark orange for [105, 135[sector.

7 DWM validation

7.1 Results for 16D spacing

All DWM validation results –provided in the following sections for 16D and 10.2D spacing– are normalized with the measured 10 m/s freestream loads (in accordance with the normalization for the freestream results in Figures 4 to 6).

Figure 10 shows the blade root flapwise bending moment DEL for an SN-slope of m = 10. The upper graph represents all measured loads. The graph in the middle represents a weighting for the wind direction (the simulated loads are weighted to represent the unequally distributed measured loads per wind direction). The lower graph shows a correction for seasonal effects (applying a weighting for winter/autumn and summer/spring periods that correlate with different turbulence intensity levels).

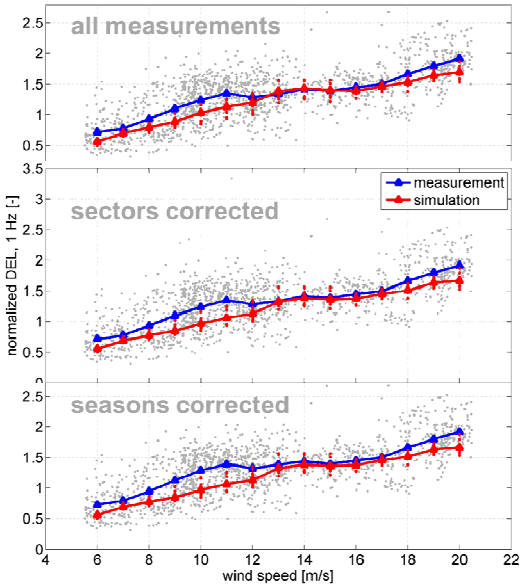

Figure 10: **16D – Blade fatigue load**
Blade root flapwise bending moment DEL (m = 10), DWM simulation vs measurement. Measured 10-min time series are grey dots, their mean values are blue. Simulated loads are red.
Upper graph: all measured loads,
Middle graph: adds a wind direction weighting,
Lower graph: adds a season weighting.

The lowest Figure with all corrections applied represents a good agreement for the low wind speeds and wind speeds above rated. There is an underestimation of the measured DEL by the DWM simulation in the partial load region.

The DEL results for the 16D spacing tower base fore-aft moment are presented in Figure 11 for an SN-slope of m = 4.
The upper Figure represents all measured loads. The Figure in the middle represents a weighting for the wind direction and the season, as specified for the blade results in Figure 10. Looking at the results of the 360° measured wake loads in Section 8, it can be concluded that there is a wake interaction from 7D. Thus, the measured loads are limited to a smaller sector (wake centre ±3°) in the lowest graph.
An underestimation of the tower bending moment can be observed in the simulation in the partial load region.

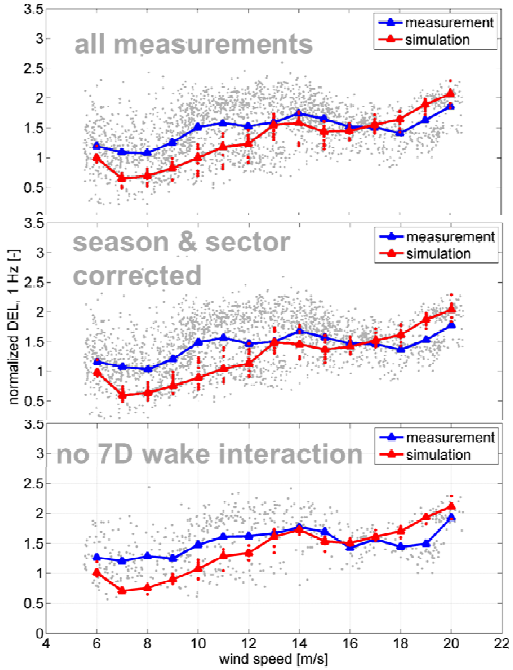

Figure 11: **16D – Tower fatigue load**
Tower bottom fore-aft moment DEL (m = 4), DWM simulation vs measurement.
Measured 10-min time series are grey dots, their mean values blue, simulated loads red.
Upper graph: all measured loads,
Middle graph: corrects wind direction and season,
Lower graph: leaves out measured loads with wake interaction from 7D.

The DEL differences between DWM simulation and model may be explained by:

a) an underestimation of the DWM model for large turbine spacings
b) DWM simulation input assumptions: Simulation input uncertainties with a significant load impact are the turbulence intensity and the vertical wind shear. For both parameters mean value assumptions are used (Sections 6 and 7). This is because the actual wind conditions (those at the time instants of the load measurements) could not be obtained, as the met mast is in wake for the 120°direction (Fig. 2).
c) a wake interaction from 7D that may superimpose onto the 16D loads of the blade. Due to a gap in blade load measurements, the sector could not be narrowed as it was done for the tower loads as specified in Figure 11 lower graph.

7.2 Results for 10.2D spacing

The wake load validation results for a spacing of 10.2D are given in Figure 12 for the blade. Again, all loads are normalized with the measured 10 m/s freestream loads. The 10.2D blade load validation shows all measured (blue) and simulated (red) loads with corrective weightings applied for the wind direction and the season, as specified in the Chapter 7 introduction.

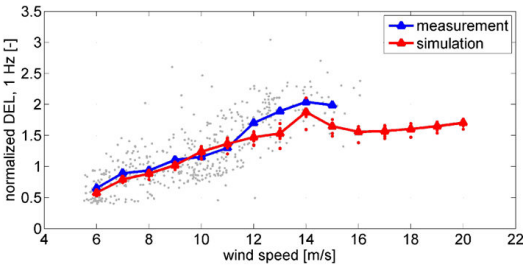

Figure 12: **10.2D – Blade fatigue load**:
Blade root flapwise bending moment DEL (m = 10), DWM simulation vs measurement, wind direction and season weightings are applied.

The tower bending moment results for a spacing of 10.2D show a significant deviance between measured (blue) and simulated (red) loads in Figure 13. Again, corrective weightings for the wind direction and the season are already applied.

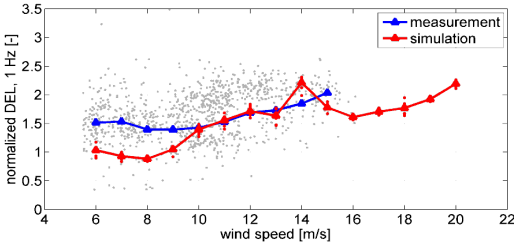

Figure 13: **10.2D – Tower fatigue load**
Tower bottom fore-aft bending moment DEL (m = 4). DWM simulation vs measurement. Wind direction and season corrections are applied

7.2.1 Influence of the atmospheric stability

As the atmospheric stability classes strongly correlate with turbulence intensity and vertical wind shear, a stability class influence study is performed. For a limited amount of data, stability class information is available from temperature measurements. This enables another parameter study for the tower. For the blade a stability class influence study is not possible as not enough data is available for a statistically reliable study.

To reduce the uncertainty in the turbulence and shear input assumptions, the stability class influence of the atmospheric boundary layer on the tower loads is examined. Comparing the upper graph in Figure 14 (representing all stability classes) with the lower graph (representing stable and neutral stability classes only), it can be assumed that the deviance between simulation and measurement correlates with unstable conditions that go along with much higher turbulence intensities than those used as simulation input.
As a result, comparing the simulation (with turbulence and shear assumptions, see Chapter 6.1) with measurements in stable and neutral conditions shows a conservative representation of the tower bottom fore-aft bending moment DEL by the DWM simulation in 10.2D spacing. This result needs further validation with more data.

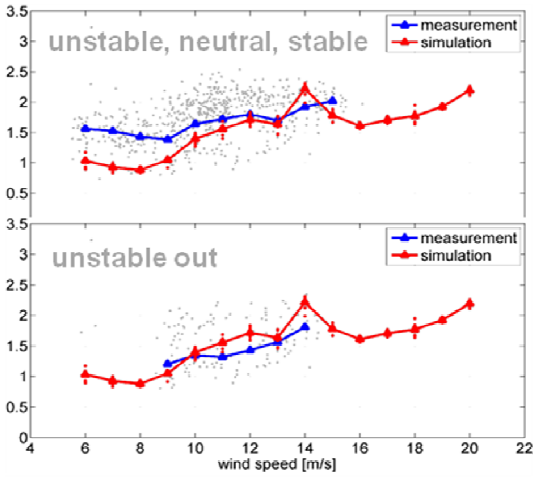

Figure 14: **10.2D – Tower fatigue load**
Stability class influence
Tower bottom fore-aft bending moment DEL (m = 4). DWM simulation vs measurement. Wind direction and season corrections are applied.
Upper graph: measured loads with atmospheric boundary layer identification.
Lower graph: measured loads with neutral or stable conditions, only.

8 Measured wake loads

The measured AV7 1 Hz fatigue loads for a 360° view around turbine AV7 are given in Figure 15 for the mean wind speed of 8 m/s ±0.5 m/s. The upper graph provides the blade root flapwise bending moment DEL (m = 10), the lower graph the tower bottom fore-aft bending moment DEL (m = 4). The loads are normalized with the mean freeflow load. The wake creating turbines are indicated by dotted lines, providing the distances from them to the wake load receiving turbine AV7 in rotor diameters D.

The graphs reveal two important findings:

a) Wake loads are still significant above a spacing of 10D, for example:
   a. there is a load increase in a 16D wake of about 70% compared to freeflow conditions for the blade root flapwise bending moment and
   b. increases of 120% for a 10.2D and 70% for a 16D wake for the tower bottom fore-aft bending moment DEL.

   This is especially important as it is common practice to consider wake loads up to a spacing of 10D, only. This mainly concerns site-specific on and offshore wind turbine, support structure and foundation design and its certification. An exemption is the recently released GL 2012 Offshore Wind Guideline [16] that states that wake load impact shall be considered for a spacing of up to 20D.

b) Two assumptions of the effective turbulence intensity approach [14] – that also form the base of its variants in the IEC edition 3 Standard [3], the Amendment 1 to that Standard as well as the GL On- [17] and Offshore [16] Wind Guidelines – seem to be confirmed.
   In detail, the alpha ventus AREVA M5000-116 blade and tower load measurement results confirm:
   a. the assumption that interacting wake loads mainly superimpose linearly
   b. the assumption that the closest wake load dominates

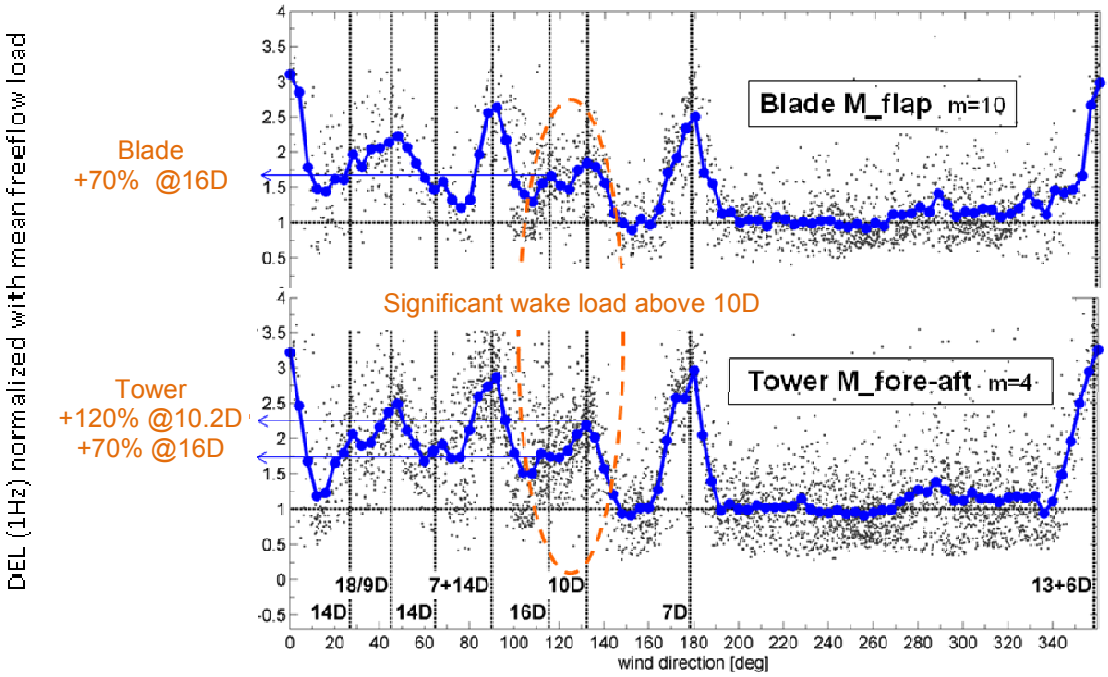

Figure 15: Measured 1 Hz fatigue loads for a 360° view around turbine AV7, wind speed of 8 m/s ±0.5 m/s.
Upper graph: Blade root flapwise bending moment DEL (m = 10).
Lower graph: Tower bottom fore-aft bending moment DEL (m = 4).

9 Conclusion

A full-scale fatigue load validation has been performed for freeflow and wake conditions with thoroughly calibrated alpha ventus AREVA M5000-116 blade and tower load measurement data.

The freeflow load validation with the Bladed software shows a good agreement for the blade root flapwise and the tower bottom overturning moments – if turbulence and wind shear are represented adequately. The DWM load validation for 16 rotor diameters (D) spacing is arguable. The differences between simulation and measurement may be caused by:

a) a turbulence underestimation within the DWM simulation input or
b) a DWM model inadequacy for very large spacings.

On the other hand, a good agreement between measured and simulated fatigue load components is given for the relatively large spacing of 10.2D. This confirms the full-scale load validations in [12] and [10] for lower spacings. The 10.2 and the 16D wake load validations rely on the same turbulence input assumptions. As the 10.2 results are better than the 16D results this may be an indication that a DWM model adjustment is advised for spacings larger than 10D.

Concerning on- and offshore wind farms, the closest spacing is mostly below 10D. The closest spacing dominates the wake loads. This is confirmed by 2 years of fully calibrated 360° freestream and wake load measurements at an AREVA M5000-116 turbine in the alpha ventus offshore wind farm. These measurements also reveal that wake loads can be quite significant above a spacing of 10D. This contrasts the common standard approach of the industry, consultants and certification agents to consider wake loads up to a spacing of 10D, only. Using the effective turbulence intensity approach as recommended in the IEC Standards [3], [18] and the GL Guidelines [16], [17]; this has a minor effect if lower spacings of the 8 surrounding turbines superimpose these large spacings from the sides [1].
But, proceeding the effective turbulence intensity approach, caution is advised if spacings larger than 10D are not superimposed by lower spacings but are left out in favor of freestream conditions. For application of the DWM model –and instead of using freestream conditions in the effective turbulence approach– this advises to use spacings of up to 20D for wake load determination. In conclusion, adjustments that introduce conservatism seem to be advised for spacings between 10 and 20D until further full-scale validations show a better agreement between simulated and measured fatigue loads than reported herein.

The DWM model can be considered ready for evaluation against the effective turbulence model which might lead to a refined design process with a positive economic impact. It is noteworthy that presently the DWM model is discussed for inclusion in the edition 4 of the IEC 61400-1 Standard that is planned to be published in 2015.

Additional notes
It should be noted that the turbulence level for the 120° direction (the direction of the 10.2 and 16D wake) is particularly low (from about 5.5 to 4% for wind speeds from 6 to 20 m/s, see Figure 9). The 120° turbulence level is low not only in comparison to other directions within the wind farm alpha ventus, but also compared to other, North or Baltic sea offshore wind farms and even lower compared to onshore wind farm turbulence levels.

Relating turbulence levels to wake loads, low turbulence will generally create less equalisation of the wind speed deficit of turbine 1 (wake creator) while meandering downstream towards turbine 2 (wake receiver). This is because turbulences “smear out” the wind speed deficit while meandering downstreams.

Concluding, the relative load increase from freestream conditions is particularly high. In result, the wake load increases pictured in the present study for 10.2 and 16D spacings may be considered as relatively conservative in comparison to larger ambient turbulence levels – if those are at comparable spacings (10, 16D).

9.1 Recommendation for further research

The yaw torsion load should be subject of further DWM validations and the validations for blade and tower loads at 10.2 D spacing should be ensured by additional data. The DWM model applicability range above 10D spacing should be validated by additional data if no factor is introduced to ensure conservatism above 10D spacing.

The DWM optimisation potential should be determined with a comparison to the effective turbulence intensity approach; initial studies have been performed by the author.

ACKNOWLEDGEMENTS

The authors gratefully acknowledge the support of all organizations and individuals who contributed to the development, the calibration and the validation of the DWM model and the data collection and calibration in alpha ventus. Their work is deemed significantly important in its contribution to future wind energy cost reduction and offshore support structure design optimisation in particular.

A great part of this work has been carried out in the OWEA LOADS and the OWEA project within the RAVE research framework funded by the German Federal Ministry for Environment BMU and the EU TOPFARM research project. The contributions from the BMU and the EU are greatly acknowledged.

REFERENCES

[1] B. Schmidt et. al. “Wake Loads and Fatigue Load Certification in Offshore Wind Farms”, Offshore EWEA proceedings, Dec. 2011.

[2] G.C. Larsen, H.Aa. Madsen, T.J. Larsen, and N. Trolborg, "Wake modeling and simulation". Risø-R-1653(EN), 2008.

[3] IEC 61400-1, International Standard, "Wind turbines – Part 1: Design requirements". 3rd edition, p.73 ff., 2005.

[4] G.C. Larsen, H.Aa. Madsen, K. Thomsen, and T.J. Larsen, "Wake meandering - a pragmatic approach". Wind Energy 11, p. 377-395, 2008.

[5] H.Aa. Madsen, G.C. Larsen, T.J. Larsen, R. Mikkelsen and N. Troldborg, "Calibration and validation of the dynamic wake meandering model implemented in the aeroelastic code HAWC2". submitted for publication in Journal of Solar Energy Engineering, 2009.

[6] T.J. Larsen, G.C. Larsen, H.Aa. Madsen and K. Thomsen, "Comparison of design methods for turbines in wake". Conference proceedings (online), European Wind Energy Conference and Exhibition, Brussels (BE), 31 Marts - 3 April 2008.

[7] G.C. Larsen et. al., "Dynamic wake meandering modeling". Risø National Laboratory for Sustainable Development, DTU, Risø-R-1607(EN), 2007.

[8] H. A. Madsen et al “Calibration and Validation of the Dynamic Wake Meandering Model for Implementation in an Aeroelastic Code”. Journal of Solar Engineering, Vol.132, November 2010

[9] H. A. Madsen ”Recalibration of the DWM model to full scale array measurements”. Risø, February 2011.

[10] K. S. Hansen, “Verification of fatigue loads in wake situation“. EU research project TOPFARM, Deliverable D4.4, 2010.

[11] B. Schmidt et. al. “Load validation and comparison versus certification approaches of the Risø Dynamic Wake Meandering model implementation in GH Bladed”. EWEA proceedings, March 2011.

[12] T.J. Larsen et. al. “Evaluation of the Dynamic Wake Meandering Model for Loads and Power Production in the Egmond aan Zee Wind Farm” to be published in WIND ENERGY, John Wiley & Sons, Ltd.

[13] A. Westerhellweg et. al: “Direction dependency of offshore turbulence intensity in the German bight”. DEWEK 2010 proceedings.

[14] S. Frandsen: “Turbulence and turbulence-generated structural loading in wind turbine clusters”. Technical Report Risø-R-1188(EN), Risø-DTU, 2005.

[15] TOPFARM – Next Generation Design Tool for Optimisation of Wind Farm Topology and Operation, Publishable final activity report, January 2011.

[16] Germanischer Lloyd, Renewables Certification, “Guideline for the Certification of Offshore Wind Turbines”, Edition 2012.

[17] Germanischer Lloyd, Renewables Certification, “Guideline for the Certification of Wind Turbines”, Edition 2010.

[18] Amendment 1:2010 to IEC 61400-1, International Standard, "Wind turbines – Part 1: Design requirements". 3rd edition, 2005.